

Nuclear magnetic resonance in higher-stage graphite intercalation compounds

Riichiro Saito, Masaru Tsukada, Katuyoshi Kobayashi, and Hiroshi Kamimura

Department of Physics, Faculty of Science, University of Tokyo, Bunkyo-ku, Tokyo, 113 Japan

(Received 28 July 1986)

The theoretical results of ^{13}C nuclear magnetic resonance shifts of higher-stage graphite intercalation compounds (GIC's) are presented. In this calculation a new formalism for calculating the chemical shifts and Knight shifts for a metallic energy-band system is proposed. In this formalism the overall feature of graphite π bands and σ bands which are mixed due to the inhomogeneous c -axis charge distribution is taken into account. The calculated results show several resonant lines with different values of scalar and dipolar Knight shifts which can be assigned to the inequivalent carbon atoms due to A - B stacking and inhomogeneous c -axis charge distribution of the graphite layers. The theoretical results of the NMR shifts on the basis of the first-principles band calculations of the higher-stage GIC's are in good agreement with the observed ones.

I. INTRODUCTION

Nuclear magnetic resonance (NMR) of graphite intercalation compounds (GIC's) has provided much information on physical quantities, serving as a microscopic probe of electronic structure of specified atoms. The information obtained by the NMR shift includes the degree of charge transfer from the intercalants studied by Carber with ^{133}Cs Knight shifts,¹ high-temperature phase transitions by Chabre *et al.* with ^{13}C and ^{81}Rb NMR,² a carbon-carbon bond length by Miller *et al.* with ^{13}C NMR,³ and the c -axis charge distribution of graphite layers by many experimental groups.⁴⁻¹¹ An interesting feature of GIC's is the inhomogeneous distribution of charges transferred from donor-type intercalants over graphite layers along the c axis. Actually, most of charges transferred from the intercalants exist on the graphite layers adjacent to the intercalant layers which we call bounding layers, and the remaining small fraction of charges exists on the interior layers. The stage dependence of various physical quantities is closely related to the c -axis charge distribution. Thus the precise determination of charge distribution has been investigated both in theory and experiment.

Theoretically the c -axis charge distribution was calculated by many groups with use of semiclassical Thomas-Fermi approximation,^{12,13} or tight binding scheme.^{14,15} A crucial factor determining a small amount of charges in the interior layers is the polarization of π bands due to screening effects. This is caused by the band mixing with core σ bands¹⁴ and antibonding π^* bands.¹⁵ Avoiding the ambiguity of the adjustable parameters used in the conventional semiempirical theory, nonempirical calculations were performed by Ohno *et al.*¹⁶⁻¹⁸ on the basis of the local-density fundamental formalism. In this calculation they adopted a thin-film model where a system consists of n graphite layers bounded by the intercalant charged sheets. They showed that the c -axis charge distribution is extremely inhomogeneous. The c -axis charge distribution in the semiempirical calculation¹²⁻¹⁵ is less inhomogeneous than that by Ohno *et al.*

Experimentally the c -axis charge distribution can be estimated by NMR experiments. Suganuma *et al.* measured the ^{13}C NMR for several donor- and acceptor-type GIC's and discussed the results in terms of heterogeneous charge distribution model.⁴ Conard *et al.* observed two ^{13}C NMR lines from graphite bounding layer and some graphitic signals of interior layers in the high field ^{13}C NMR.^{5,6} However, a powdered sample used in these experiments results in much broadened signals due to the large anisotropic parts of NMR shifts of graphite and GIC's as two-dimensional materials. Recently high resolution ^{13}C NMR in highly oriented pyrolytic graphite (HOPG) has enabled us to make sophisticated measurements of NMR signal from inequivalent carbon atoms in graphite layers.^{2,3} Domignetz *et al.*⁷ and Kume *et al.*⁸⁻¹¹ showed independently that the ^{13}C NMR spectra of higher-stage GIC's consist of several lines at room temperature. Furthermore, Kume *et al.* determined the distribution of density of states at the Fermi level from ^{13}C spin-lattice relaxation time T_1 of an individual resolved line.^{10,11} According to Kume *et al.* the c -axis charge distribution is less inhomogeneous than that predicted by Ohno and Kamimura¹⁷ in case of potassium GIC's. From the assignment of observed resonant lines to the inequivalent carbon atoms by Kume *et al.* each inequivalent graphite layer yields a doublet resonant line which has a different value in a shift for a different inequivalent graphite layer. The origin of the appearance of a doublet line for a graphite layer is different for the first and higher-stage GIC's as follows.^{7,11} In the first stage the appearance of a doublet line can be explained from the fact that two kinds of carbon atoms exist according to the distance from intercalant atoms which form a 2×2 superlattice relative to a graphite lattice. In the higher stage GIC's, on the other hand, the local environment of carbon atoms is averaged out due to the rapid motion of alkali-metal atom in higher stage GIC's.⁷ Thus the existence of a doublet line in higher-stage GIC's is ascribed to the inequivalency of carbon atoms due to A - B layer stacking.

Though information on charge distribution is obtained from the shift and width of a NMR line in the high-

resolution NMR experiments, the charge distribution was determined from T_1 , that is, the width of a NMR line. The reason for this is that the shift of a NMR line consists of the chemical shifts and Knight shifts which include information on charge density, and it is very difficult to determine chemical and Knight shift separately.

Theoretically the chemical shifts of GIC's was calculated by Tsang and Resing using the tight-binding approximation for a two-dimensional graphite band.¹⁹ They calculated the paramagnetic (Ramsey) intra-atomic term from the contributions at only three symmetry points of Brillouin zone. The dipolar term was estimated from the Fermi-level density of states $N(E_F)$ obtained by specific-heat experiments. They claimed that the paramagnetic shift does not change by intercalation and that the reduction of anisotropy of NMR shifts upon intercalation is due to the increase of dipolar shifts. As regards the anisotropy of the shift for a field direction, the dipolar shift has an opposite sign to paramagnetic shift. However the appearance of several lines in high-resolution NMR spectra of higher stage GIC's can not be explained by the single-graphite-layer model, because all carbon atoms are equivalent within the two dimensional graphite bands. Moreover the σ - π mixing, which is missing in the single graphite layer model influences significantly the Knight shift because it is caused by the nonzero $2s$ component in $N(E_F)$ induced by this mixing. In this view the precise calculation of chemical shifts and Knight shifts should be done, using the more realistic band calculation. Especially since the c -axis charge distribution is determined by the screening due to the σ - π mixing, the relation between the σ - π mixing and NMR gives important information about the charge distribution.

The purpose of the present paper is to calculate the chemical shifts and Knight shifts for inequivalent carbon sites of higher-stage GIC's nonempirically. For this aim, we first develop a theoretical formulation for calculating the diamagnetic and paramagnetic chemical shifts and scalar and dipolar Knight shifts. This formulation is presented in Sec. II. In Sec. III we calculate numerically

the chemical shifts and the Knight shifts for inequivalent carbon atoms from second-stage to sixth-stage GIC's with charge transfer $f=1.0$. The calculation is based on the band structure derived by Ohno and Kamimura. Theoretical results of $f=1.0$ are compared with NMR experimental results in Sec. IV. Through the analysis of numerical results, we try to clarify the effect of c -axis charge distribution to the shifts. In Sec. V main results obtained in this paper are summarized.

II. FORMULATION FOR MAGNETIC SHIELDING TENSOR

In NMR, the resonance field at a nucleus in a bulk is different from that of a free nucleus. If we denote the shift of the total field seen by $\Delta\mathbf{H}$, the relative resonance frequency shift σ which is independent of H is defined in a tensor form by

$$\Delta\mathbf{H} = -\sigma \cdot \mathbf{H}, \quad (1)$$

where σ is called the shielding tensor. There are two kinds of contributions to the shielding tensor; one from the orbital motion of electrons around a nucleus and the other from the electron and nucleus spin-spin interactions, which are called chemical shifts and Knight shifts of NMR, respectively. Chemical shifts and Knight shifts are further decomposed into diamagnetic and paramagnetic shifts, and scalar and dipolar Knight shifts, respectively.¹⁸ Hereafter we call only scalar Knight shift as Knight shift and dipolar Knight shift as dipolar shift for simplicity. As a result the shielding tensor consists of the following four components which originate from different interactions between a nucleus and electrons and they are completely independent of each other,^{18,20}

$$\sigma = \sigma^{(p)} + \sigma^{(d)} + \sigma^{(D)} + \sigma^{(K)}. \quad (2)$$

Here $\sigma^{(p)}$, $\sigma^{(d)}$, $\sigma^{(D)}$, and $\sigma^{(K)}$ are the shielding tensor corresponding to paramagnetic, diamagnetic, dipolar and Knight shifts, respectively, which are expressed in terms of one-electron wave function ψ_i as,

$$\sigma^{(p)} = \frac{e^2}{2m^2c^2} \sum_{j,j'} 2 \frac{\langle \psi_j | \frac{1}{r^3} | \psi_{j'} \rangle \langle \psi_{j'} | 1 | \psi_j \rangle + \langle \psi_{j'} | \frac{1}{r^3} | \psi_j \rangle \langle \psi_j | 1 | \psi_{j'} \rangle}{E_{j'} - E_j}, \quad (3)$$

$$\sigma^{(d)} = \frac{e^2}{2mc^2} \sum_j 2 \left\langle \psi_j \left| \frac{r^2 \mathbf{I} - \mathbf{r}\mathbf{r}}{r^3} \right| \psi_j \right\rangle, \quad (4)$$

$$\sigma^{(D)} = \sum_j \left[-\frac{(\gamma e \hbar)^2}{2} \frac{\partial f(E)}{\partial E} \Big|_{E_j} \right] \left\langle \psi_j \left| \frac{r^2 \mathbf{I} - 3\mathbf{r}\mathbf{r}}{r^5} \right| \psi_j \right\rangle, \quad (5)$$

$$\sigma^{(K)} = -\frac{8\pi}{3} \sum_j \left[-\frac{(\gamma e \hbar)^2}{2} \frac{\partial f(E)}{\partial E} \Big|_{E_j} \right] \langle \psi_j | \delta(\mathbf{r}) | \psi_j \rangle. \quad (6)$$

In the above expressions, e , m , γ_e , c , and $f(E)$ are the charge, the mass, gyromagnetic ratio of the electron, velocity of light, and the Fermi distribution function, respectively, and the summation on j is taken over occupied one-electron states with the energy E_j and j' over unoccupied states with the energy $E_{j'}$. In these equations spin degeneracy is included. When one electron wave functions ψ_j are expanded in terms of atomic orbital ϕ_v ,

$$\psi_j = \sum_{\nu} a_{\nu j} \phi_{\nu}, \quad (7)$$

Eqs. (3)–(6) are expressed as

$$\sigma^{(p)} = -\frac{e^2}{2m^2c^2} \sum_{\mu\nu} \sum_{\lambda\rho} K_{\mu\nu,\rho\lambda}^{(p)} \left[\left\langle \phi_{\nu} \left| \frac{1}{r^3} \right| \phi_{\mu} \right\rangle \left\langle \phi_{\lambda} | 1 | \phi_{\rho} \right\rangle + \left\langle \phi_{\lambda} \left| \frac{1}{r^3} \right| \phi_{\rho} \right\rangle \left\langle \phi_{\nu} | 1 | \phi_{\mu} \right\rangle \right] \quad (8)$$

with

$$K_{\mu\nu,\rho\lambda}^{(p)} = \sum_{j,j'} \frac{2a_{\nu j}^* a_{\mu j'} a_{\lambda j'}^* a_{\rho j}}{E_{j'} - E_j} \\ = 4 \int_{-\infty}^{E_F} dE \int_{E_F}^{\infty} dE' \frac{\rho_{\lambda\mu}(E') \rho_{\nu\rho}(E)}{E' - E}, \quad (9)$$

$$\sigma^{(d)} = \frac{e^2}{2mc^2} \sum_{\nu,\mu} K_{\nu\mu}^{(d)} \left\langle \phi_{\nu} \left| \frac{\nu^2 I - \mathbf{r}\mathbf{r}}{r^3} \right| \phi_{\mu} \right\rangle, \quad (10)$$

with

$$K_{\nu\mu}^{(d)} = \sum_j 2a_{\nu j}^* a_{\mu j} = 2 \int_{-\infty}^{E_F} \rho_{\nu\mu}(E) dE, \quad (11)$$

$$\sigma^{(D)} = \sum_{\nu,\mu} K_{\nu\mu}^{\text{sp}} \left\langle \phi_{\nu} \left| \frac{r^2 I - 3\mathbf{r}\mathbf{r}}{r^5} \right| \phi_{\mu} \right\rangle, \quad (12)$$

and

$$\sigma^{(K)} = -\frac{8\pi}{3} \sum_{\nu,\mu} K_{\nu\mu}^{\text{sp}} \langle \phi_{\nu} | \delta(\mathbf{r}) | \phi_{\mu} \rangle, \quad (13)$$

with

$$K_{\nu\mu}^{\text{sp}} = \sum_{\nu,\mu} \left[-\frac{(\gamma_e \hbar)^2}{2} \frac{\partial f(E)}{\partial E} \Big|_{E_j} \right] a_{\nu j}^* a_{\mu j} \\ = \int \left[-\frac{(\gamma_e \hbar)^2}{2} \frac{\partial f(E)}{\partial E} \right] \rho_{\nu\mu}(E) dE = \frac{(\gamma_e \hbar)^2}{2} \rho_{\mu\nu}(E_F). \quad (14)$$

In the above, we introduced the density matrix $\rho_{\mu\nu}$ defined as

$$\rho_{\mu\nu} = \sum_j \delta(E - E_j) a_{\mu j}^* a_{\nu j}. \quad (15)$$

Equations (8)–(14) are a general formula for the NMR shielding tensor in any energy band system. The local information of the wave functions around a nucleus is expressed as the matrix elements pertinent to the atomic orbitals and the information of an energy band structure is included in the density matrix $\rho_{\mu\nu}(E)$. For the basis functions ϕ_{ν} 's and density matrix $\rho_{\nu\mu}$, we adopted those of LCAO scheme used by Ohno and Kamimura.¹⁷ As the angular part of atomic orbitals, the components of $s(l=0)$, p_x , p_y and $p_z(l=1)$ of a carbon atom are taken into account. Contributions of higher spherical harmonics are small. When we consider only intra-atomic terms in the calculation of matrix elements of ϕ_{ν} , Eqs. (8)–(14) can be written as

$$\sigma^{(i)} = \begin{pmatrix} \sigma_{\perp}^{(i)} & 0 & 0 \\ 0 & \sigma_{\perp}^{(i)} & 0 \\ 0 & 0 & \sigma_{\parallel}^{(i)} \end{pmatrix} \quad (i=p,d,D,K), \quad (16)$$

with

$$\sigma_{\perp}^{(p)} = -\frac{e^2 \hbar^2}{2m^2 c^2} 2P_3 (K_{xzzx}^{(p)} + K_{zxzx}^{(p)}), \quad (17)$$

$$\sigma_{\parallel}^{(p)} = -\frac{e^2 \hbar^2}{2m^2 c^2} 2P_3 2K_{xxxx}^{(p)}, \quad (18)$$

$$\sigma_{\perp}^{(d)} = \frac{e^2}{2mc^2} \left[\frac{2}{3} S_1 K_{ss}^{(d)} + \frac{2}{5} P_1 (3K_{xx}^{(d)} + 2K_{zz}^{(d)}) \right], \quad (19)$$

$$\sigma_{\parallel}^{(d)} = \frac{e^2}{2mc^2} \left[\frac{2}{3} S_1 K_{ss}^{(d)} + \frac{2}{5} P_1 (4K_{xx}^{(d)} + K_{zz}^{(d)}) \right], \quad (20)$$

$$\sigma_{\perp}^{(D)} = \frac{2}{5} P_3 (K_{zz}^{\text{sp}} - K_{xx}^{\text{sp}}), \quad (21)$$

$$\sigma_{\parallel}^{(D)} = \frac{4}{5} P_3 (K_{xx}^{\text{sp}} - K_{zz}^{\text{sp}}), \quad (22)$$

$$\sigma_{\perp}^{(K)} = \sigma_{\parallel}^{(K)} = -\frac{8}{3} \pi K_{ss}^{\text{sp}} |R_{2s}(0)|^2, \quad (23)$$

where

$$S_1 = \left\langle R_{2s} \left| \frac{1}{r} \right| R_{2s} \right\rangle, \quad (24)$$

$$P_1 = \left\langle R_{2p} \left| \frac{1}{r} \right| R_{2p} \right\rangle, \quad (25)$$

$$P_3 = \left\langle R_{2p} \left| \frac{1}{r^3} \right| R_{2p} \right\rangle. \quad (26)$$

Furthermore, R_{2s} and R_{2p} are the radial parts of $2s$ and $2p$ wave functions of a carbon atom in a crystal, which are obtained by solving the atomic LDF equations self-consistently. These formula have been derived using threefold symmetry with regard to the rotation around each carbon atom. By this symmetrized property the matrix elements of the shielding tensor are expressed by the quantities S_1 , P_1 , P_3 , $\rho_{ss}(E)$, $R_{2s}(0)$, $\rho_{xx}(E)$, and $\rho_{zz}(E)$ for each carbon site. These quantities are numerically calculated with use of the results of the first-principles band calculations by Ohno and Kamimura. The value of ρ_{ss} , ρ_{xx} , and ρ_{zz} are usually called as the partial density states of $2s$, $2p_x$, and $2p_z$ components of the bands, respectively. Numerical integration of these parameters and the calculation of shielding tensor are done by a supercomputer S810 in the University of Tokyo with a fine care of accuracy. It should be noted that the calculation of $K_{\mu\nu,\rho\lambda}^{(p)}$ in Eq. (9) should be done carefully since the integrand of Eq. (9) diverges at $E=E'=E_F$. We find that the integration does not diverge even at $E=E'=E_F$ as far as $\rho_{\mu\nu}$ is finite.

TABLE I. Calculated results of NMR shifts for inequivalent carbon sites from second- to sixth-stage GIC's with the charge transfer $f = 1.0$. The graphite layers are labeled consequently, starting with layer 1, the bounding layer.

Layer (site)		NMR shifts				Total (ppm)
		Diamagnetic (ppm)	Paramagnetic (ppm)	Dipole (ppm)	Knight (ppm)	
Stage 2						
1 α	σ_{\perp}	57.9	-332.3	13.9	-8.7	-269.2
	σ_{\parallel}	57.8	-219.8	-27.8	-8.7	-198.6
	σ_{iso}	57.9	-294.8	0.0	-8.7	-245.6
	σ_a	-0.2	112.4	-41.7	0.0	70.6
1 β	σ_{\perp}	58.6	-332.9	13.1	-22.0	-283.3
	σ_{\parallel}	58.3	-221.7	-26.2	-22.0	-211.6
	σ_{iso}	58.5	-295.8	0.0	-22.0	-259.4
	σ_a	-0.2	111.2	-39.3	0.0	71.6
Stage 3						
1 α	σ_{\perp}	59.2	-337.7	18.3	0.7	-259.5
	σ_{\parallel}	58.8	-222.5	-36.6	0.7	-199.6
	σ_{iso}	59.1	-299.3	0.0	0.7	-239.5
	σ_a	-0.4	115.2	-54.9	0.0	59.9
1 β	σ_{\perp}	59.2	-341.8	18.3	0.0	-264.2
	σ_{\parallel}	58.8	-226.6	-36.7	0.0	-204.5
	σ_{iso}	59.1	-303.4	0.0	0.0	-244.3
	σ_a	-0.4	115.2	-55.0	0.0	59.8
2 α	σ_{\perp}	59.2	-342.6	4.0	-23.8	-303.3
	σ_{\parallel}	59.0	-222.1	-7.9	-23.8	-194.8
	σ_{iso}	59.2	-302.5	0.0	-23.8	-267.1
	σ_a	-0.2	120.5	-11.9	0.0	108.5
2 β	σ_{\perp}	59.4	-343.0	4.1	-52.9	-332.4
	σ_{\parallel}	59.2	-222.1	-8.2	-52.9	-223.9
	σ_{iso}	59.4	-302.7	0.0	-52.9	-296.2
	σ_a	-0.3	121.0	-12.3	0.0	108.5
Stage 4						
1 α	σ_{\perp}	59.8	-344.9	20.5	1.0	-263.6
	σ_{\parallel}	59.3	-229.8	-41.0	1.0	-210.5
	σ_{iso}	59.6	-306.5	0.0	1.0	-245.9
	σ_a	-0.5	115.3	-61.4	0.0	53.2
1 β	σ_{\perp}	59.8	-347.5	20.5	0.5	-266.8
	σ_{\parallel}	59.3	-232.2	-41.0	0.5	-213.4
	σ_{iso}	59.5	-309.1	0.0	0.5	-249.0
	σ_a	-0.5	115.3	-61.5	0.0	53.4
2 α	σ_{\perp}	59.5	-350.3	5.1	-14.1	-299.7
	σ_{\parallel}	59.4	-228.2	-10.3	-14.1	-193.2
	σ_{iso}	59.5	-309.6	0.0	-14.1	-264.2
	σ_a	-0.1	122.0	-15.4	0.0	106.5
2 β	σ_{\perp}	59.7	-350.3	5.3	-29.9	-315.7
	σ_{\parallel}	59.6	-228.5	-10.7	-29.9	-209.5
	σ_{iso}	59.7	-310.1	0.0	-29.9	-280.3
	σ_a	-0.2	122.4	-16.0	0.0	106.3
Stage 5						
1 α	σ_{\perp}	60.0	-347.4	19.5	0.9	-267.1
	σ_{\parallel}	59.3	-229.3	-39.0	0.9	-208.1
	σ_{iso}	59.7	-308.1	0.0	0.9	-247.5
	σ_a	-0.6	118.1	-58.6	0.0	59.0

TABLE I. (Continued).

Layer (site)		NMR shifts				Total (ppm)
		Diamagnetic (ppm)	Paramagnetic (ppm)	Dipole (ppm)	Knight (ppm)	
1 β	σ_{\perp}	59.9	-350.3	19.5	0.2	-270.6
	σ_{\parallel}	59.3	-232.0	-39.1	0.2	-211.5
	σ_{iso}	59.5	-310.9	0.0	0.2	-250.9
	σ_a	-0.6	118.4	-58.6	0.0	59.1
2 α	σ_{\perp}	59.6	-348.3	4.1	-13.5	-298.0
	σ_{\parallel}	59.3	-225.8	-8.2	-13.5	-188.1
	σ_{iso}	59.5	-307.4	0.0	-13.5	-261.4
	σ_a	-0.3	122.5	-12.4	0.0	109.9
2 β	σ_{\perp}	59.7	-347.9	4.5	-28.6	-312.2
	σ_{\parallel}	59.4	-225.3	-9.0	-28.6	-203.4
	σ_{iso}	59.6	-307.0	0.0	-28.6	-276.0
	σ_a	-0.3	122.6	-13.5	0.0	108.8
3 α	σ_{\perp}	59.9	-348.6	0.7	0.0	-288.1
	σ_{\parallel}	59.8	-227.1	-1.4	0.0	-168.8
	σ_{iso}	59.8	-308.1	0.0	0.0	-248.3
	σ_a	-0.0	121.5	-2.1	0.0	119.3
3 β	σ_{\perp}	59.2	-346.5	1.5	-0.6	-286.3
	σ_{\parallel}	59.1	-226.8	-3.0	-0.6	-171.4
	σ_{iso}	59.2	-306.6	0.0	-0.6	-248.0
	σ_a	-0.1	119.6	-4.6	0.0	114.9
Stage 6						
1 α	σ_{\perp}	60.2	-344.1	23.1	1.2	-259.7
	σ_{\parallel}	59.6	-228.2	-46.1	1.2	-213.5
	σ_{iso}	60.0	-305.5	0.0	1.2	-244.3
	σ_a	-0.6	116.0	-69.2	0.0	46.2
1 β	σ_{\perp}	60.1	-346.9	23.1	0.6	-263.0
	σ_{\parallel}	59.6	-230.6	-46.1	0.6	-216.5
	σ_{iso}	60.0	-308.1	0.0	0.6	-247.5
	σ_a	-0.5	116.2	-69.2	0.0	46.5
2 α	σ_{\perp}	59.6	-347.2	6.9	-18.2	-298.9
	σ_{\parallel}	59.5	-227.5	-13.7	-18.2	-199.9
	σ_{iso}	59.6	-307.3	0.0	-18.2	-265.9
	σ_a	-0.1	119.6	-20.6	0.0	99.0
2 β	σ_{\perp}	59.8	-347.2	7.0	-37.9	-318.3
	σ_{\parallel}	59.7	-227.8	-13.9	-37.9	-220.0
	σ_{iso}	59.7	-307.4	0.0	-37.9	-285.6
	σ_a	-0.1	119.4	-20.9	0.0	98.3
3 α	σ_{\perp}	60.0	-351.1	4.9	-0.4	-286.5
	σ_{\parallel}	60.0	-231.4	-9.8	-0.4	-181.6
	σ_{iso}	60.0	-311.2	0.0	-0.4	-251.6
	σ_a	-0.0	119.6	-14.7	0.0	104.9
3 β	σ_{\perp}	59.4	-348.9	5.4	-1.3	-285.3
	σ_{\parallel}	59.3	-230.9	-10.8	-1.3	-183.7
	σ_{iso}	59.4	-309.5	0.0	-1.3	-251.4
	σ_a	-0.1	117.9	-16.2	0.0	101.6

III. CALCULATED RESULTS OF NMR SHIFTS

In Table I we present the calculated results of NMR shifts for inequivalent carbon sites from second to sixth stage GIC's with charge transfer $f=1.0$. We list the shift

for an applied field along the c axis, σ_{\parallel} , that perpendicular to the c axis, σ_{\perp} , the isotropic component of the shift, $\sigma_{\text{iso}} [=(\sigma_{\parallel}+2\sigma_{\perp})/3]$, and anisotropic component $\sigma_a [=(\sigma_{\parallel}-\sigma_{\perp})]$. Further in this table the contribution from diamagnetic, paramagnetic, dipolar and Knight shifts are

also shown for $\sigma_{||}$, σ_{\perp} , σ_{iso} , and σ_a . The graphite layers are labeled consecutively, starting with layer 1 being the bounding layer. In every graphite layer there are two inequivalent carbon atoms due to A - B stacking of graphite layers which are denoted by α and β as illustrated by black and white circles in Fig. 1. Neighboring atoms exist (do not exist) right above and below α - (β -) type atom along the c axis in the adjacent graphite layer.

A. Diamagnetic shift

Diamagnetic shifts for all carbon atoms from second stage to sixth stage with $f=1.0$ have a nearly constant value of about 60 ppm and they are almost isotropic except for a small anisotropy in fraction of 1 ppm. The small anisotropy of diamagnetic shifts is due to the slight difference of the occupation numbers between $2p_{x,y}$, and $2p_z$ orbitals, that is the difference between the values of $K_{xx}^{(d)}$ and $K_{zz}^{(d)}$ in Eqs. (19) and (20). There are two reasons for this difference. One is that the extra charge in the antibonding π^* band transferred from donor type intercalants enhances K_{zz} , but not K_{xx} . The other is the polarization effect of the bonding σ and π bands by the charged intercalant layers. Since the bonding σ electrons are coupled with bonding or antibonding π bands by polarization effects, the occupation number of $2s$ and $2p_{x,y}$ in bonding σ bands are deviated about the order 10^{-2} from that of the sp^2 configuration. Typical occupation number of $2s$ and $2p_x$ orbitals are 1.02 and 0.99, respectively. In spite of a small value of σ - π mixing ratio, this effect is important in order to determine the c -axis charge distribution. The polarization effect contributes also significantly to the Knight shift as shown later in this section. It is noted that the polarization effect may be more important than the effect of transferred charge for the diamagnetic shift especially in the case of higher stage GIC's since the anisotropy of diamagnetic shift still exists even in the interior layer with a small excess charge.

Important information on the diamagnetic shift we should point out here based on our calculations is the contribution of $1s$ electrons of carbon atoms to the diamagnetic shift. The $1s$ electron does not contribute to other NMR shifts because the $1s$ orbital forms a very deep closed shell. From the value of $\langle r^{-1} \rangle_{1s} = 5.6116$ a.u. calculated by a numerical basis carbon $1s$ orbital, the contri-

bution to the diamagnetic shift from $1s$ electrons is estimated to be 199.2 ppm. Since the value of $\langle r^{-1} \rangle$ for $1s$ is much larger than that for $2s$, $\langle r^{-1} \rangle_{2s} = 0.903$ a.u., and that for $2p$, $\langle r^{-1} \rangle_{2p} = 0.789$ a.u., the $1s$ electrons contribute dominantly to the diamagnetic shift. Therefore the diamagnetic shift is isotropic and does not change with changing the stage number.

B. Paramagnetic shift

Paramagnetic shift of GIC's has the largest absolute value among others and it determines the sign of the total shifts. Typical values of $\sigma_{\perp}^{(p)}$, $\sigma_{||}^{(p)}$ and its anisotropy are about 340, 225, and 115 ppm, respectively. The absolute value of paramagnetic shift does not change so much by the stage number. The reason for this, proposed by Tsang *et al.*,¹⁹ within the rigid band model of two-dimensional graphite is as follows. The contribution of $\sigma_{||}$ comes from excitation between bonding σ and antibonding σ^* bands which does not have partial density of states near the Fermi level. Thus there is little effect of the staging on the paramagnetic term of $\sigma_{||}$. In Fig. 2 the partial density of states in the case of second stage are shown for the easy understanding of the relative position of these bands. In this figure the σ bands are further decomposed into the $2s$ orbital component and the $2p_x$ and $2p_y$ orbital components. Concerning σ_{\perp} , the contribution comes from sum of the excitations between occupied π and unoccupied σ^* bands, and occupied σ and unoccupied π^* bands which are expressed as $K_{zz}^{(p)}$ and $K_{zzxx}^{(p)}$ in Eq. (17). We might expect a significant stage dependence of σ_{\perp} due to the charge transfer effect, since the important contribution to paramagnetic shift comes from the integration near the Fermi level. However such an effect for σ_{\perp} turns out to be small. The reason is that the enhancement of π - σ^* excitation due to the Fermi level shift to the σ^* band is compensated by the decrease of σ - π^* excitation.

The above discussion is valid even in the case of higher-stage GIC's because the paramagnetic shift is contribution from the entire Brillouin zone. Nevertheless one observes clearly in the calculated results, in Table I, a small, but significant effect of the charge transfer which comes from the modification at small part of energy bands near E_F . For example, in the case of the third stage, the paramagnetic shift of site α of layer 1, that is, the bounding layer, is 4.0 ppm larger than that of site β in the same layer. Though this difference is small compared with the absolute value of the shift, it gives the most important contribution to the difference between site α and β in the total shift as shown in Table I. An explanation of this effect on the paramagnetic shift is obtained from the detailed band structure near E_F . In the n stage GIC's there are n conduction bands and n valence bands which consist of $2p_z$ orbitals of carbon atoms of n graphite layers. If we neglect interlayer interactions between graphite layers, each conduction and valence bands are composed with an equal weight of the atomic orbitals of site α and site β in a graphite layer. Taking account of the interlayer interactions, the components of Bloch orbitals of site α and β in the same energy bands are not equal. The dominant contribution to this effect comes from inter-

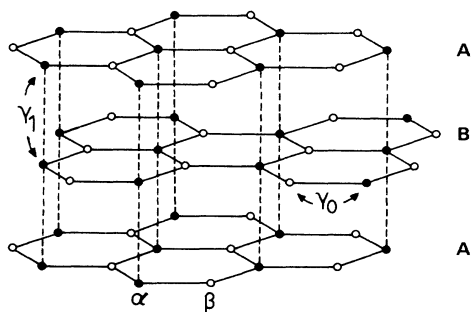


FIG. 1. A - B stacking of graphite layers. γ_0 and γ_1 are the transfer integrals between some neighbor carbon atoms.

layer interaction γ_1^{21} , which represents the transfer integral between one carbon atom and the other sitting just above or below it. Because of the *A-B* stacking as shown in Fig. 1, only the Bloch orbitals of site α can interact with each other by γ_1 . As a result, the interlayer interaction γ_1 lifts the degeneracy of the conduction bands and the valence bands on the equivalent graphite layers. The split bands which have different energy relative to Fermi energy contribute differently to the partial density of states of site α and β . This causes the difference of paramagnetic shifts between site α and β . Though the energy bands in the higher stage are more complex than those in the lower stage because of many interlayer interactions between graphite layers, the difference of paramagnetic shift between site α and β in the same graphite layer can be explained by the relative energy position with regard to E_F of the split bands with the different orbital components of site α and β . For example, in the case of paramagnetic shifts for interior layers the difference of paramagnetic shift of site α and β in fifth and

sixth stage has an opposite sign to the case of lower stage or the bounding layers. For the interior layers of higher stage GIC's, the excess charge from donor-type intercalants is so small that the large part of these energy bands are situated above the Fermi level. Therefore the energy bands which belong to site α is nearer to the Fermi level than those which belong to site β and thus the paramagnetic shift of site α is larger than that of site β .

C. Dipolar shift and Knight shift

Dipolar shift and Knight shifts in the present calculation give important information on the electronic structure of metallic π^* bands of every graphite layer, since they yield different values of shifts for inequivalent carbon sites. These shifts come from the electron spin polarization in a magnetic field. Since the density of electron spin is proportional to the density of states for each π^* band at the Fermi level $N(E_F)$, the shifts have different values due to the inhomogeneous *c*-axis distribution of charges transferred from intercalants. Though both shifts are due to the electron spin, they are related to the spin densities of the different atomic orbitals in different manner. Dipolar shift is related mainly to $2p$ orbitals through classical dipole-dipole interactions between a nuclear spin and an electron spin. This interaction is anisotropic and thus there is no isotropic term in the dipolar shift. Though the dipolar shift comes mostly from the π electrons, all contributions from $2s$ and $2p$ orbitals to the shifts are included in the present calculation. On the contrary, the Knight shift is related only to the s orbital. In spite of a small component of $2s$ orbital in $N(E_F)$, this interaction is large enough to produce a significant isotropic shift. We can obtain information on the s -orbital admixture in π bands from the value of the Knight shift. This mixing effect is important in determining the *c*-axis charge distribution, as reviewed in Sec. I.

For the second stage, the absolute value of the dipolar shift is $\sigma_{\parallel}^{(D)} = 13$ ppm and $\sigma_{\perp}^{(D)} = -27$ ppm, and its anisotropy is 40 ppm. Since the sign of anisotropy of dipolar shift is opposite to that of paramagnetic shift, the anisotropy of total shift becomes small. Further the magnitude of the dipolar shift is increased by the electron donation from the alkali-metal intercalants. This causes the reduction of anisotropy of ^{13}C -NMR shift from graphite to GIC's. In the third stage the π^* bands which belong to the carbon sites of the interior layer have smaller $N(E_F)$ than the π^* bands of the bounding layer due to the inhomogeneous *c*-axis charge distribution.²¹ Therefore the dipolar shifts of site 2α and 2β in the interior layer are smaller than those of site 1α and 1β in the bounding layer. For higher-stage GIC's, by the same reason, the anisotropy of total shift becomes larger as going from the bounding layer to the interior layer.

The magnitude of the Knight shift in the second stage takes different values for the site 1α and 1β . The difference is so large that two NMR peaks of the corresponding sites can be resolved. Detailed analysis of numerical data shows that $2s$ component in $N(E_F)$ through the π^* - σ^* band mixing effect induces the Knight shift. The mixing ratio of these bands becomes larger near the crossing re-

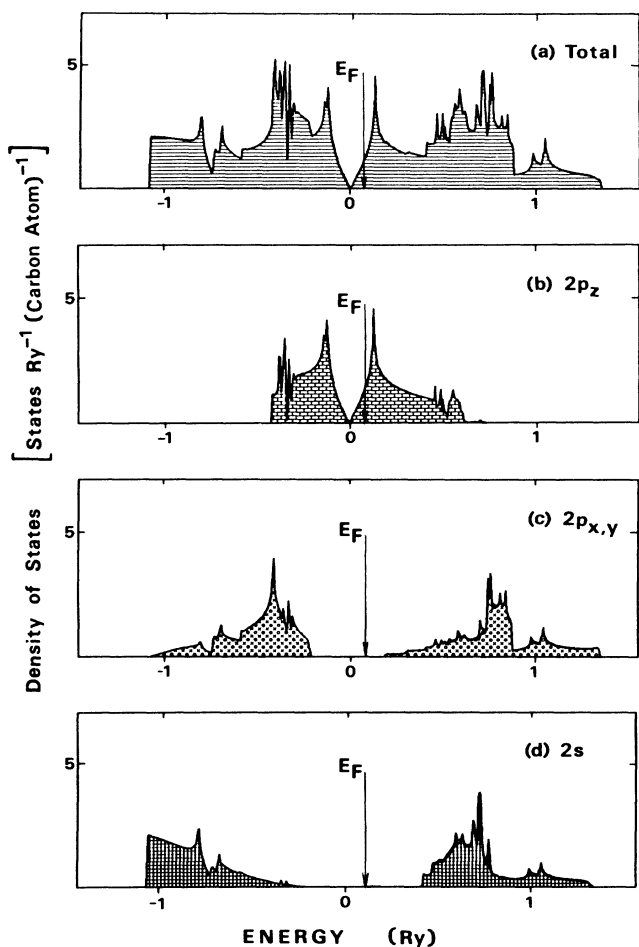


FIG. 2. Density of states of graphitic energy bands for the second stage GIC; (a) total density of states, and partial density of states of (b) $2p_z$, (c) $2p_x$ or $2p_y$, and (d) $2s$ components of carbon atomic orbitals.

gion of π^* and σ^* bands between Γ and K points of the Brillouin zone.¹⁷ Therefore the relative $2s$ component in $N(E_F)$ is large in the interior layers compared with the bounding layer. Further the $2s$ component of π^* band is larger in site β than in site α in the same graphite layer. The reason for that is explained as follows. Since the π^* band of site α gains the additional energy γ_1 due to the interlayer interaction as compared with that of site β , the $2s$ component of π^* band in site α is smaller than in site β .

In the higher stage GIC's, the Knight shift has a larger value for interior layers and a smaller value for bounding layers. This fact can also be explained by the relative position of π^* bands to σ^* band. In the fifth and sixth stages, however, the Knight shift of the innermost layers has an exceptionally small value in spite of strong σ^* - π^* coupling. The reason for this is that the density of states at the Fermi level $N(E_F)$ of the innermost graphite layer is very small because of extreme inhomogeneous c -axis charge distribution.

IV. COMPARISON WITH EXPERIMENTS AND DISCUSSION

In this section we compare calculated results of anisotropy of shift σ_a and of resonance peak positions for the case of $\mathbf{H}\perp c$ axis with experimental results by Kume *et al.* for stages 2, 3, 4, and 6. In Table II we compare the anisotropy of total shift of the present results σ_a with the experimental one. As seen in Table II the agreement between theory and experiment is good. As discussed above, the anisotropy of the total shift has a close relation to the electronic structure of π bands, and the dominant contribution to the anisotropy is the paramagnetic shift which reflects global features of π band. Therefore the anisotropy of shift is not so sensitive to the c -axis charge distributions.

On the other hand, the absolute value of the shifts is very sensitive to a slight change of charge transfer, especially in interior layers because a little change in character of $2s$ orbital affects the Knight shift appreciably. From this standpoint we have calculated the absolute value of

TABLE II. Comparison of the anisotropy of the total shift of the present results with the experimental results (Ref. 10).

Stage	Site	Present results	Experimental results
2	1 α	70.6	53
	1 β	71.6	67
3	1 α	59.9	62
	1 β	60.0	65
	2 α	108.5	139
6	2 β	108.5	144
	1 α	46.2	90
	1 β	46.5	91
	2 α	99.0	167
	2 β	98.0	144
	3 α	104.9	134
	3 β	101.6	134

the shift for the case of $\mathbf{H}\perp c$, σ_{\perp} . In Fig. 3 we indicate the calculated NMR peak positions corresponding to σ_{\perp} . For comparison the observed resonance peak positions in the high resolution ^{13}C spectra of K GIC's by Kume *et al.* for the case of $\mathbf{H}_0\perp c$ axis, where the standard signal of tetramethylsilane (TMS) is assumed as -76 ppm with inclusion of the diamagnetic shift of $1s$ electrons. As seen in the figure, the calculated stage dependence of σ_{\perp} reproduces well the observed trend. By this calculation it has been shown for the first time that peak 1a in the experimental signal corresponds to the site β of the layer 1 (bounding layer), and 1b corresponds to site α of the same layer. For other graphite layers the assignment of peak a to α site and peak b to β site is also made. As regards the third stage the fact that the difference between 2a and 2b is larger than that between 1a and 1b can be explained by the contribution of Knight shift, because the difference between the site α and β is due to the Knight shift. It should be further noticed that the relative value of the calculated shifts for layer 2 to those for layer 1 is much larger than that of the experiment. This tendency can be also seen in the higher-stage GIC's. Since the difference of shift at 2 α and 2 β in the calculated results is almost the same as the difference of observed 2a and 2b, the discrepancy between theory and experiment lies in the difference between the shifts of layer 1 and 2. Since the difference between the layer 1 and 2 is due to the dipolar effect, we can make the distribution of the transferred π electrons less inhomogeneous over different layers without changing its $2s$ component, the agreement between the theory and experiment will be improved. In order to re-

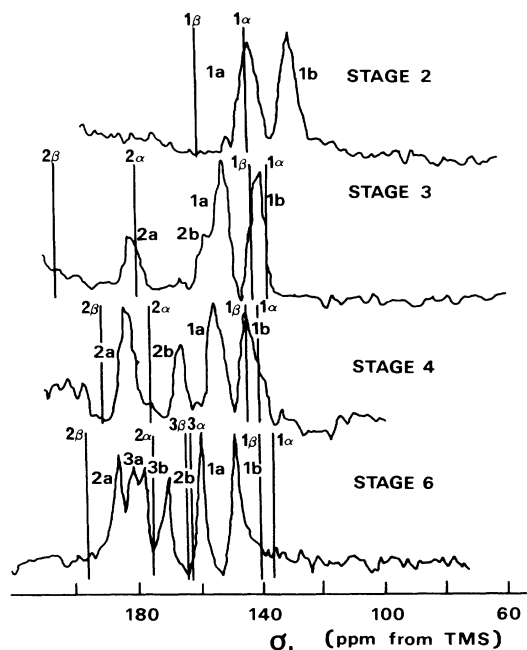


FIG. 3. Comparison of the absolute values of σ_{\perp} of the present results with those of the experiment by Kume *et al.* (Ref. 10), assuming the absolute value of TMS as -76 ppm.

move the discrepancy between theory and experiments, we need use more sophisticated nonempirical band calculations. In the Ohno-Kamimura's calculation the transfer interaction between graphite layers through the intercalant layers has been neglected. If this interaction is taken into account, we expect that the *c*-axis charge distribution will be less inhomogeneous, because the strong attractive interaction between positive intercalated layers and negative bounding layers becomes weak by screening effects.

V. CONCLUSION

In conclusion we have calculated the chemical shifts and Knight shifts at inequivalent carbon sites in higher-stage GIC's on the basis of the first-principles band calculation. In doing so, we have developed a new formulation to calculate the shielding tensor for the NMR frequency shift in metallic systems. The numerical calculations have been performed for donor-type GIC's from the second to sixth stage with charge transfer $f=1.0$. We have calculated four kinds of the shift (diamagnetic, paramagnetic, dipolar, and Knight shifts) separately for a ^{13}C nuclear spin in inequivalent carbon sites, and clarified how each of these four kinds of mechanism contribute to chemical and Knight shifts of GIC's. We have shown especially, that the dipolar shift and Knight shift play important roles in determining the resonance frequency position observed in ^{13}C NMR experiments of higher-stage GIC's. We have further shown that the absolute value and aniso-

tropy of the NMR shift are determined mainly by the paramagnetic shift and diamagnetic shift and that the difference of anisotropy for inequivalent carbon sites is due to the dipolar shift. The calculated anisotropy of the shifts at inequivalent carbon sites in various graphite layers for each stage of higher-stage GIC's has reproduced the observed values fairly well. We have also shown that the stage dependence of the absolute values of shielding tensor has reproduced the observed tendency satisfactorily well. Finally we have suggested that in order to obtain quantitative agreement between theory and experiment in the case of donor-type GIC's the charge distribution must be less inhomogeneous compared with that obtained by Ohno and Kamimura and thus a band-structure calculation in a more realistic system than the thin-film model adopted by Ohno and Kamimura is necessary.

ACKNOWLEDGMENTS

We would like to thank Dr. Takahisa Ohno for variable discussions and providing the program of band calculations. We also express our gratitude to Dr. N. Shima for helpful suggestion and discussion. We also thank Professor K. Kume and his co-workers, and Professor T. Kondow for sending the detailed experimental data and valuable discussions. Part of this work was supported by the grants-in-aid of special research project on properties of molecular assemblies (No. 60104002) from the Ministry of Education, Science and Culture, Japan.

¹G. P. Carber, *Phys. Rev. B* **2**, 2284 (1970).

²Y. Chabre, P. Segransan, C. Berthier, F. J. DiSalvo, and J. E. Fischer, *Synth. Met.* **8**, 7 (1983).

³G. R. Miller, C. F. Poranski, Jr., and H. A. Resing, *J. Chem. Phys.* **80**, 1708 (1984).

⁴M. Suganuma, U. Mizutani, and T. Kondow, *Phys. Rev. B* **22**, 5079 (1980).

⁵J. Conard, M. Gutierrez-Le Brun, P. Langinie, H. Estrade-Szwarcckopf, and G. Herman, *Synth. Met.* **2**, 227 (1980).

⁶J. Conrad, P. Lauginie, H. Estrade-Szwarcckopf, G. Hermann, D. Guerard, and P. Lagrange, *Physica* **105B**, 285 (1981).

⁷D. D. Dominguez, H. A. Resing, C. F. Poranski, Jr., and J. S. Murday, *Mater. Res. Soc. Symp. Proc.* **20**, 363 (1983).

⁸K. Kume and Y. Maniwa, *Synth. Met.* **6**, 219 (1983).

⁹K. Kume, Y. Maniwa, H. Suematsu, and S. Tanuma, *Solid State Commun.* **47**, 537 (1983).

¹⁰K. Kume, Y. Maniwa, S. Tanuma, Y. Iye, and H. Suematsu, *Synth. Met.* **8**, 69 (1983).

¹¹Y. Maniwa, K. Kume, H. Suematsu, and S. Tanuma, *J. Phys. Soc. Jpn.* **54**, 666 (1985).

¹²L. Pietronero, S. Strassler, H. R. Zeller, and M. J. Rice, *Phys. Rev. Lett.* **41**, 763 (1978).

¹³S. A. Aafran and D. R. Hamman, *Phys. Rev. B* **22**, 606 (1980).

¹⁴S. A. Safran and D. R. Hamman, *Phys. Rev. B* **23**, 565 (1981).

¹⁵S. Shimamura and A. Morita, *J. Phys. Soc. Jpn.* **51**, 502 (1982).

¹⁶T. Ohno, N. Shima, and H. Kamimura, *Solid State Commun.* **44**, 761 (1982).

¹⁷T. Ohno and H. Kamimura, *J. Phys. Soc. Jpn.* **52**, 228 (1983).

¹⁸C. P. Slichter, *Principle of Magnetic Resonance* (Springer, Berlin, 1978), Chap. 4.

¹⁹T. Tsang and H. A. Resing, *Solid State Commun.* **53**, 39 (1985).

²⁰M. Karplus and T. P. Das, *J. Chem. Phys.* **34**, 1683 (1961).

²¹R. Saito and H. Kamimura, *Phys. Rev. B* **33**, 7218 (1986).